

Femtoscopy of stopped protons

Andrzej Bialas,^{1,*} Adam Bzdak,^{2,†} and Volker Koch^{3,‡}

¹*M. Smoluchowski Institute of Physics, Jagellonian University, Lojasiewicza 11, 30-348 Kraków, Poland*

²*AGH University of Science and Technology, Faculty of Physics and Applied Computer Science, 30-059 Kraków, Poland*

³*Nuclear Science Division, Lawrence Berkeley National Laboratory, Berkeley, California 94720, USA*



(Received 9 December 2017; revised manuscript received 27 December 2018; published 15 March 2019)

The longitudinal proton-proton femtoscopy (Hanbury Brown–Twiss) correlation function, based on the idea that in a heavy-ion collision at $\sqrt{s} \lesssim 20$ GeV stopped protons are likely to be separated in configuration space, is evaluated. It shows a characteristic oscillation which appears sufficiently pronounced to be accessible in experiment. The proposed measurement is essential for estimating the baryon density in the central rapidity region and can be also viewed as an (almost) direct verification of the Lorentz contraction of the fast-moving nucleus.

DOI: [10.1103/PhysRevC.99.034906](https://doi.org/10.1103/PhysRevC.99.034906)

I. INTRODUCTION

The search for a possible phase structure of QCD has been a focus point in strong interaction research. Lattice QCD calculations have established that for vanishing and small net-baryon density the transition from hadrons to quarks and gluons is an analytic crossover [1]. The situation at larger baryon density, on the other hand, is less clear, since at present lattice methods cannot access this region because of the fermion sign problem. Here one has to rely on model calculations and a large class of these models do indeed predict a first-order phase coexistence region which ends in a critical point (see, e.g., Ref. [2] for an overview).

In order to explore the region of large net-baryon density experimentally, one studies heavy-ion collisions at moderate beam energies $\sqrt{s} \lesssim 20$ GeV, where a sufficient amount of the incoming nucleons are stopped at midrapidity in order to achieve the necessary baryon density. Indeed, since produced baryons always come as baryon-antibaryon pairs, the only means of producing a finite net baryon density is by stopping the nucleons of the colliding nuclei. Thus, in order to explore the QCD phase diagram at large baryon density, the question of baryon stopping is essential to understand. In fact, stopping the baryons is only a necessary condition. In addition to being at midrapidity in momentum space, they also need to overlap in configuration space.

The mechanism by which the incoming nucleons are stopped is indeed a very interesting question [3–8]. However, independent of the specific mechanism, it seems rather

unphysical that the nucleons are stopped instantaneously. Instead, it will take time and space for the nucleons to decelerate. Therefore, it is rather unlikely that the stopped nucleons will end up at $z \simeq 0$, i.e., at the point of the collision of the two nuclei. Instead, one would expect that the nucleons from the right-going nucleus will end up at positions in configuration space with $z > 0$ and the left-going ones at $z < 0$ so that the stopped nucleons may actually be distributed bimodally in configuration space. This observation was recently pointed out in Ref. [9]. Based on a simple string model, Ref. [9] found that for collision energies $\sqrt{s} \gtrsim 10$ GeV the stopped nucleons actually will not overlap significantly in configuration space. Of course, this observation was based on a rather simple model and it would be much better if this observation could be verified or ruled out in experiments. This is the purpose of this paper, where we propose to measure *longitudinal* Hanbury Brown–Twiss (HBT)–type correlations (also known as femtoscopy [10]) of the stopped protons, i.e., protons at $y_{cm} \approx 0$ with transverse momentum not exceeding, say, 1 GeV. Since femtoscopy does not *a priori* distinguish between stopped and produced protons, it is important to choose a collision energy which is small enough for proton production to be negligible but sufficiently high so that the deceleration length is large enough for the stopped protons to be separated in configuration space. Thus an energy of $\sqrt{s} \simeq 20$ GeV appears to be a good choice since at this energy the antiproton to proton ratio is still very small, $\bar{p}/p \simeq 0.1$ [11,12].

This paper is organized as follows: In the next section, we present and discuss the source function based on the same simple string model used in Ref. [9] (corrected, however, for the Fermi motion inside a nucleus). Next, we calculate the resulting femtoscopy correlation function before we close with a discussion of the various issues and limitations of this study.

II. THE SOURCE FUNCTION

The essential ingredient for femtoscopy is the underlying source of the emitted particles, protons in our case. The source

*bialas@th.if.uj.edu.pl

†bzdak@fis.agh.edu.pl

‡vkoch@lbl.gov

Published by the American Physical Society under the terms of the [Creative Commons Attribution 4.0 International](https://creativecommons.org/licenses/by/4.0/) license. Further distribution of this work must maintain attribution to the author(s) and the published article's title, journal citation, and DOI. Funded by SCOAP³.

is the phase-space distribution of emission points, which are typically the points of the last interaction of the protons before they fly to the detector. Clearly a quantitative calculation of such a source function would require a sophisticated simulation. However, we believe that certain semiquantitative aspects can be discussed without such a treatment, and it is this approach we will take in the following.

As already eluded to in the introduction, once two nucleons collide it is very unlikely or possibly even unphysical for them to come to a stop right at the collision point. Instead, they will only come to a stop after a certain distance and time.

The distance Δz and time Δt between the collision and the final space-time point (z, t) where and when a nucleon acquires its final rapidity y depends on the mechanism of deceleration and thus on the model used for its description. It is in general a function of the initial and final rapidity, Y_i and y , as well as the typical transverse mass, M_\perp , the nucleon acquires after the collision.

For a given collision space-time point (z_c, t_c) in the center-of-mass frame of the two nucleons, we thus have

$$\begin{aligned} z &= z_c \pm \Delta z(Y_i, y, M_\perp), \\ t &= t_c + \Delta t(Y_i, y, M_\perp), \end{aligned} \quad (1)$$

where the plus sign refers to the right-going particles and the minus sign to the left-going ones.

One sees from (1) that, in order to construct the source needed for femtoscopy, we need a distribution of the collision points in space and time and a model or theory which determines Δz and Δt .

A. Distribution of collision points

Let us start with the collision point distribution. Here, we follow Ref. [9] and assume that the distribution of nucleons inside the target and projectile nuclei can be reasonably described by a Gaussian. In this case, the longitudinal (z -direction) and transverse components of the collision point distribution factorize and subsequently we will concentrate on the collision point distribution in the z direction, which, following Ref. [9], we assume to be proportional to the overlap of the distribution of the nucleons in the left- and right- moving nuclei.

We thus have

$$W_c(z_c, t_c) \sim e^{-\gamma^2[z_c - \zeta_L(t_c)]^2/R_L^2} e^{-\gamma^2[z_c - \zeta_R(t_c)]^2/R_R^2} \Theta(t_c), \quad (2)$$

where

$$\zeta_L(t) = -\zeta_R(t) = \zeta_0 - Vt; \quad \zeta_0 \gg R_{L,R}/\gamma, \quad (3)$$

are the positions of the centers of the nuclei at the time t . ζ_0 and $-\zeta_0$ are positions of the centres of left-moving and right-moving nuclei at $t = 0$ before the nuclei have any contact with each other. This implies $\zeta_0 \gg R_{L,R}/\gamma$ and $t_c \geq 0$. Also, $\gamma = \cosh(Y_{cm})$ denotes the Lorentz contraction factor for the incoming nuclei in the center-of-mass frame, which we are working in.

B. Distribution of nucleon emission points z and t

Consider first the right-movers. For the distribution of z and t , we have

$$\begin{aligned} W_R(z, t) &= \int dz_c dt_c W_c(z_c, t_c) \delta(z - z_c - \Delta z) \delta(t - t_c - \Delta t) \\ &\sim e^{-\gamma^2[z - \Delta z - Z]^2/R_L^2} e^{-\gamma^2[z - \Delta z + Z]^2/R_R^2} \Theta(t - \Delta t) \end{aligned} \quad (4)$$

with $Z \equiv \zeta_0 - V(t - \Delta t)$.

For left-movers, the formula differs by the sign of Δz :

$$W_L(z, t) \sim e^{-\gamma^2[z + \Delta z - Z]^2/R_L^2} e^{-\gamma^2[z + \Delta z + Z]^2/R_R^2} \Theta(t - \Delta t). \quad (5)$$

For identical nuclei, we have

$$\begin{aligned} W(z, t; P_i, P_f) &= W_L(z, t) + W_R(z, t) \sim (e^{-[z + \Delta z]^2/\Gamma_c^2} + e^{-[z - \Delta z]^2/\Gamma_c^2}) \\ &\times e^{-Z^2/\Gamma_c^2} \Theta(t - \Delta t), \end{aligned} \quad (6)$$

where $\zeta_0 \gg R/\gamma$, $\Gamma_c^2 = R^2/2\gamma^2$, and the dependence on the initial and final momenta is implicit via Δz and Δt .

What remains then is to determine Δz and Δt . For nucleons with small transverse velocities, the simplest model is that of linear energy loss, as for instance used in the Lund model [13] or the Bremsstrahlung model [14]. Using the conditions¹

$$dE/dz = \sigma, \quad dP/dt = \sigma, \quad (7)$$

where σ denotes the energy loss per unit length or string tension, one obtains [9]

$$\Delta z(P_i, P_f, \sigma) = \frac{E_i - E_f}{\sigma}, \quad E_f = M_\perp \cosh y, \quad (8)$$

$$\Delta t(P_i, P_f, \sigma) = \frac{P_i - P_f}{\sigma}, \quad P_f = M_\perp \sinh y. \quad (9)$$

Here $P_i = M \sinh(Y_i)$, $E_i = \sqrt{M^2 + P_i^2}$, and $P_f = M_\perp \sinh(y)$, $E_f = \sqrt{M_\perp^2 + P_f^2}$ are the initial and final longitudinal momenta and energies.

These equations determine Δz and Δt for initial and final longitudinal momenta, P_i and P_f , transverse mass of the final proton, M_\perp , and for a given rate of energy loss σ (string tension). In reality, the string tension is not a constant but may fluctuate from collision to collision (e.g., depending on number of constituent quarks wounded in a given collision). Since it is unlikely, however, that a nucleon with only one or two wounded quarks may fully stop, the sample of the nucleons with the final rapidity $y \approx 0$ is expected to be largely dominated by those with three wounded quarks. Thus we shall ignore fluctuations due to the string tension and take $\sigma = 3\sigma_0 = 3 \text{ GeV/fm}$. For the transverse mass, we subsequently will chose a value of $M_\perp = 1.2 \text{ GeV}$ (we verified that the results are not sensitive to the actual value of M_\perp).

¹The second condition expresses the equation of motion with the force equal to σ . It is exact when the transverse velocity of the nucleon vanishes. We have verified that for the nucleons of transverse momenta not exceeding 1 GeV the corrections are negligible.

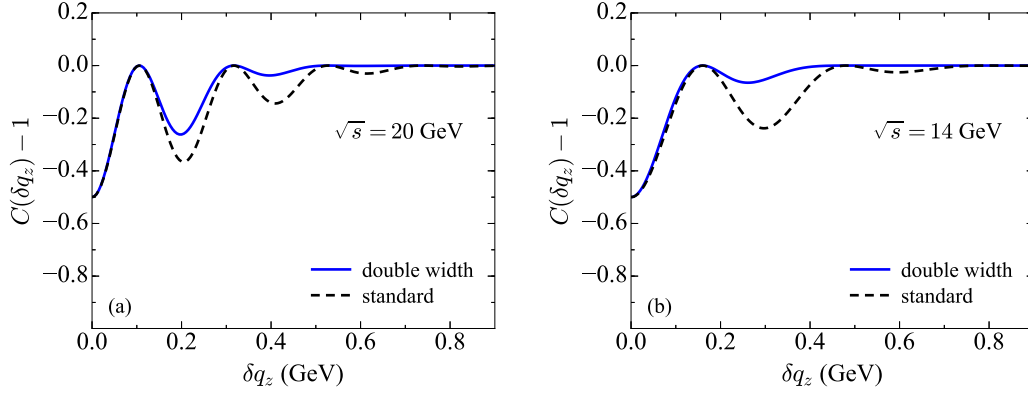


FIG. 1. Femtoscopy correlation function for (a) $\sqrt{s} = 20$ GeV and (b) $\sqrt{s} = 14$ GeV. The black dashed lines represent the result of our model calculation while the solid blue lines are obtained by doubling the value of width of the collision point distribution, Γ_c .

C. Fermi motion

In the case of a nucleus-nucleus collision, the nucleons inside the target and projectile nuclei experience Fermi motion. Consequently, the initial momentum of the colliding nucleons is distributed around the nominal (mean) value of the nucleus-nucleus collision. This broadens the emission source in the longitudinal spatial direction and thus affects the femtoscopy signal. We have

$$W_F(z, t, P_i, P_f) = \int dP_i G_F(P_i - \langle P_i \rangle) W(z, t; P_i, P_f), \quad (10)$$

where $G_F(P_i - \langle P_i \rangle)$ is the distribution of the actual initial momentum P_i of the nucleon around the average $\langle P_i \rangle$. We shall take it in the form

$$G_F(P_i - \langle P_i \rangle) \sim e^{-[P_i - \langle P_i \rangle]^2 / \Gamma_F^2},$$

$$\Gamma_F = \gamma \sqrt{\frac{2}{5}} k_F \simeq \gamma 165 \text{ MeV}, \quad (11)$$

where k_F is the Fermi momentum.² Note that due to the Lorentz boost the width of the distribution Γ_F scales with the Lorentz factor γ , $\Gamma_F \sim \gamma$. This increases substantially the width of this distribution in the energy region of interest.

III. THE HBT CORRELATION FUNCTION

The femtoscopic longitudinal correlation function we are seeking is given by [10,15]

$$C(\delta q_z; \delta q_0) - 1 = -\frac{1}{2} \frac{|\Phi(\delta q_z; \delta q_0)|^2}{|\Phi(\delta q_z = 0; \delta q_0 = 0)|^2}, \quad (12)$$

where δq_z is the difference of the longitudinal momenta of the two protons, δq_0 is the difference of their energies,

²The value of Γ_F follows from the demand that the distribution G_F exhibits the same variance as the Fermi gas with the Fermi momentum k_F . Also, we ignore the small effect of the binding energy of the nucleons and instead assume that we can treat the nucleons as free particles.

and

$$\Phi(\delta q_z, \delta q_0; P_i, P_f) = \int_{-\infty}^{\infty} dz e^{iz\delta q_z} \int_{\Delta t}^{\infty} dt e^{-it\delta q_0} W(z, t; P_i, P_f) \quad (13)$$

is the Fourier transform of the density.

Since we are working with Gaussians, the Fourier transforms are straightforward. We have

$$\Phi(\delta q_z, \delta q_0; P_i, P_f) \sim \cos[\delta q_z \Delta z] e^{-(\delta q_z \Gamma_c)^2 / 4} e^{-i\delta q_0(\Delta t + \zeta_0/V)} \times e^{-(\delta q_0 \Gamma_c)^2 / (4V^2)}, \quad (14)$$

where for the Fourier transform in t it was essential to use the condition $\zeta_0 \gg R/\gamma$ which allowed us to integrate over time from $-\infty$.

Thus, the final result for the correlation function, including Fermi motion, is

$$C_F(\delta q_z; \delta q_0) - 1 = -\frac{1}{2} \frac{|\Phi_F(\delta q_z; \delta q_0)|^2}{|\Phi_F(\delta q_z = 0; \delta q_0 = 0)|^2}, \quad (15)$$

where

$$\begin{aligned} \Phi_F(\delta q_z, \delta q_0; P_i, P_f) &= \int dP_i G_F(P_i - \langle P_i \rangle) \Phi(\delta q_z; \delta q_0; P_i, P_f) \\ &\sim e^{-\frac{\Gamma_c^2 + \Gamma_F^2 / \sigma^2}{4} (\delta q_z^2 + \delta q_0^2)} \left[\cos(\delta q_z \Delta Z) \cosh\left(\delta q_0 \delta q_z \frac{\Gamma_F^2}{2\sigma^2}\right) \right. \\ &\quad \left. + i \sin(\delta q_z \Delta Z) \sinh\left(\delta q_0 \delta q_z \frac{\Gamma_F^2}{2\sigma^2}\right) \right], \end{aligned} \quad (16)$$

where we have omitted a common phase which does not play any role in the correlation function. Here, we have assumed that the momentum dependence of the shift Δz , Eq. (8), may be approximated by

$$\begin{aligned} \Delta z &= \frac{E_i - E_f}{\sigma} = \frac{E_i - \langle E_i \rangle}{\sigma} + \frac{\langle E_i \rangle - E_f}{\sigma} \simeq \frac{P_i - \langle P_i \rangle}{\sigma} + \Delta Z; \\ \Delta Z &\equiv (\langle E_i \rangle - E_f) / \sigma, \end{aligned} \quad (17)$$

where $\langle E_i \rangle$ is the mean (nominal) energy of the incident nuclei and ΔZ denotes the shift in space for the mean energy. We fur-

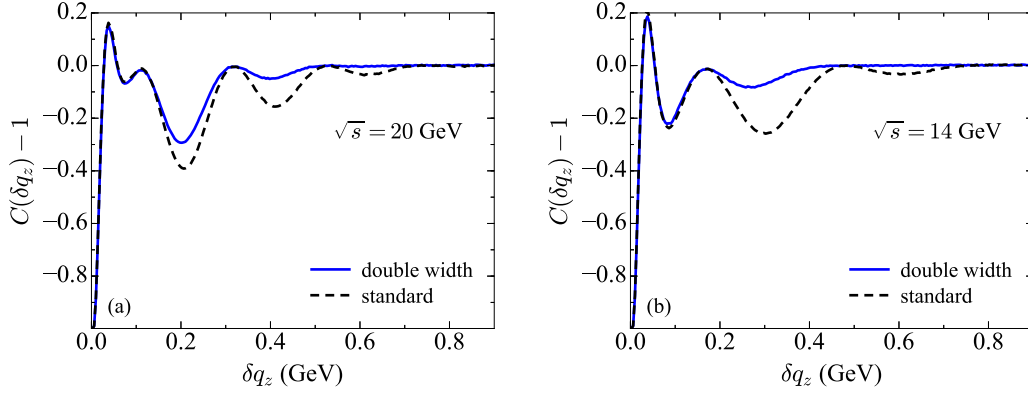


FIG. 2. Same as Fig. 1 but with strong and Coulomb interaction effects included.

ther assumed that the velocity of the nuclei in the c.m. frame is close to unity, $V \simeq 1$. For the energies under consideration, $\sqrt{s} > 10$ GeV, these should be very good approximations and indeed we find that the resulting correlation function agrees with the full result within a few per mille.

IV. RESULTS

The correlation function (15) evaluated for $\delta q_0 = 0$ (corresponding to protons with equal and opposite rapidities) is shown in Fig. 1. Here, we used for the radius $R = 7$ fm and $M_{\perp,1} = M_{\perp,2} = 1.2$ GeV. In Fig. 1(a), we show the predicted femtoscopy correlation function for a collision energy of $\sqrt{s} = 20$ GeV and in Fig. 1(b) for $\sqrt{s} = 14$ GeV. The black dashed lines represent the result for the model discussed above. The blue solid lines are the results, where we doubled the width Γ_c of the collision point distribution in order to allow for additional smearing (induced, e.g., by a nonzero proton radius not taken into account in our model). One sees characteristic oscillations of the correlation function, reflecting the two maximum structure of the source density.

To obtain experimental predictions, the correlation function seen in Fig. 1 must be corrected for the final-state interactions [16,17]. They are shown in Fig. 2 with strong and Coulomb interaction effects taken into account. One sees

that although these corrections strongly affect the very small region of δq_z , the region of δq_z where the oscillations are observed remains qualitatively unchanged.

In Fig. 3, we show the corresponding time-integrated source distribution,

$$\begin{aligned} \bar{W}(z; P_i, P_f) = \int dt W_F(z, t; P_i, P_f) \sim & \exp\left(-\frac{(z - \Delta Z)^2}{\Gamma_F^2/\sigma^2 + \Gamma_c^2}\right) \\ & + \exp\left(-\frac{(z + \Delta Z)^2}{\Gamma_F^2/\sigma^2 + \Gamma_c^2}\right). \end{aligned} \quad (18)$$

Here, we used the same approximation as before, Eq. (17).

We see that the separation of the stopped protons exhibited in the source distribution manifests itself as extra oscillation in the femtoscopy correlation function. For a collision energy of $\sqrt{s} = 20$ GeV, the signal is clearly visible for both the model result as well the more conservative result, where we doubled the width Γ_c . At $\sqrt{s} = 14$ GeV, the signal is much weaker, however.

V. CONCLUSION AND REMARKS

In conclusion, we have presented a calculation of the longitudinal femtoscopy correlation function of stopped protons based on the observation that in a heavy-ion collision

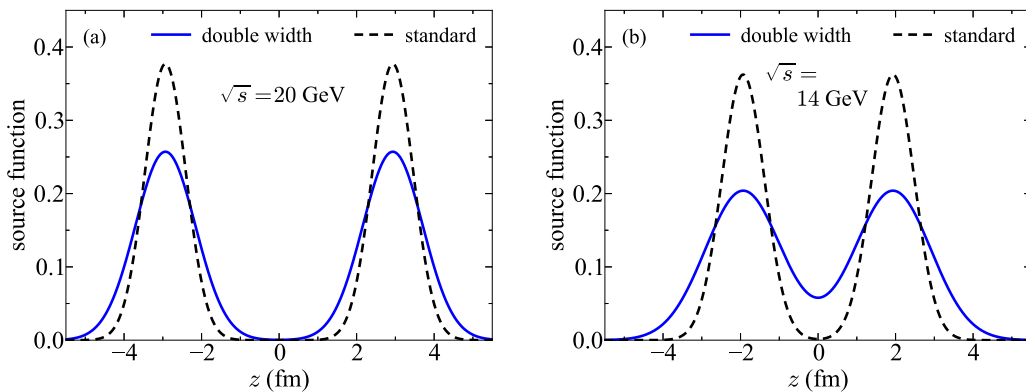


FIG. 3. Time integrated source function for stopped protons as a function of z for (a) $\sqrt{s} = 20$ GeV and (b) $\sqrt{s} = 14$ GeV. The black dashed lines represent the result of our model calculation while the blue solid lines are obtained by doubling the value of width of the collision point distribution, Γ_c . The source functions shown are normalized to unity.

at $10 \text{ GeV} \lesssim \sqrt{s} \lesssim 20 \text{ GeV}$ such protons are likely to be separated in configuration space. The resulting correlation function shows extra oscillations which appear sufficiently pronounced to be accessible in experiment. Clearly such a measurement, if feasible, would be most desirable. It will provide useful information about the longitudinal configuration space distribution of the nucleons in a heavy-ion collision, and, more importantly, it will provide essential constraints on the mechanism by which baryon number is transported to midrapidity.

Some remarks are in order:

- (i) The observation of the suggested extra oscillations will not only confirm the idea that the nucleons do not stop immediately after collision. It should also allow us to measure the effective distance at which the energy is deposited in the produced particles. Indeed, as seen from Eq. (16), Φ_F (and thus also C_F) explicitly depend on ΔZ , the average distance required to stop a proton.
- (ii) Even if the oscillations are not seen, the measurement will determine the (longitudinal) size of the volume from which the protons at $y_{cm} \approx 0$ are emitted. This should allow us to estimate the actual density of protons in configuration space, the quantity essential for the studies of this system. One also obtains the upper limit on the distance the nucleons travel before attaining the rapidity $y \approx 0$, thus improving our understanding of the process of the energy loss by the leading particles in a high-energy collision.
- (iii) The definition of the longitudinal correlation function requires that the vector $\delta\vec{q}$ points in the z direction, i.e., $\delta q_{\perp} = 0$. In our approximation of the nuclear densities as Gaussians, this restriction is not important, as the longitudinal and transverse degrees of freedom factorize. To increase statistics, one may thus integrate over transverse momenta. Since the Lund

model is best justified at small transverse velocities, and since the Gaussian form is only an approximation, it seems reasonable, however, to restrict measurements to protons with transverse momenta not exceeding, say, 1 GeV.

- (iv) It turns out that the corrections due to the Coulomb and strong interactions do not change qualitatively the possibility of observation of the expected oscillations of the correlation function.
- (v) Our calculation ignored entirely possible correlations between the outgoing protons due to quark mixing at very short distances [18]. Introducing such correlations may result in the correlation function being positive in some region of δq_z . As shown in Ref. [18], however, this effect is small and should not modify our conclusions.
- (vi) Finally, let us add that our results rely strongly on the idea that the longitudinal distribution of nucleons inside moving nucleus are Lorentz contracted and that this contraction survives during the collision. The proposed measurement should thus provide an interesting test of this effect (for the recent discussion of the measurements of Lorentz contraction, see Ref. [19]).

ACKNOWLEDGMENTS

We thank Scott Pratt for providing his code to calculate the effects of strong and Coulomb interaction effects and useful correspondence. Thanks are due to Mike Lisa for interesting discussions. This work was partially supported by the Faculty of Physics and Applied Computer Science AGH UST statutory tasks No. 11.11.220.01/1 within subsidy of Ministry of Science and Higher Education, the National Science Centre Grants No. 2014/15/B/ST2/00175 and No. 2013/09/B/ST2/00497, and the U.S. Department of Energy, Office of Science, Office of Nuclear Physics, under Contract No. DE-AC02-05CH11231.

-
- [1] Y. Aoki, G. Endrodi, Z. Fodor, S. D. Katz, and K. K. Szabo, *Nature (London)* **443**, 675 (2006).
 - [2] M. A. Stephanov, *PoS* **032**, 024 (2006).
 - [3] R. Anishetty, P. Koehler, and L. D. McLerran, *Phys. Rev. D* **22**, 2793 (1980).
 - [4] W. Busza and A. S. Goldhaber, *Phys. Lett. B* **139**, 235 (1984).
 - [5] W. Busza and R. Ledoux, *Annu. Rev. Nucl. Part. Sci.* **38**, 119 (1988).
 - [6] D. Kharzeev, *Phys. Lett. B* **378**, 238 (1996).
 - [7] A. Capella and B. Z. Kopeliovich, *Phys. Lett. B* **381**, 325 (1996).
 - [8] M. Li and J. I. Kapusta, *Phys. Rev. C* **95**, 011901 (2017).
 - [9] A. Bialas, A. Bzdak, and V. Koch, *Acta Phys. Pol. B* **49**, 103 (2018).
 - [10] M. A. Lisa, S. Pratt, R. Soltz, and U. Wiedemann, *Annu. Rev. Nucl. Part. Sci.* **55**, 357 (2005).
 - [11] L. Adamczyk *et al.* (STAR Collaboration), *Phys. Rev. C* **96**, 044904 (2017).
 - [12] T. Anticic *et al.* (NA49 Collaboration), *Phys. Rev. C* **83**, 014901 (2011).
 - [13] B. Andersson, *The Lund Model* (Cambridge University Press, Cambridge, UK, 1998).
 - [14] L. Stodolsky, *Phys. Rev. Lett.* **28**, 60 (1972).
 - [15] S. Pratt, *Phys. Rev. Lett.* **53**, 1219 (1984).
 - [16] R. Lednicky and V. L. Lyuboshits, *Yad. Fiz.* **35**, 1316 (1981) [*Sov. J. Nucl. Phys.* **35**, 770 (1982)].
 - [17] J. Adam *et al.* (ALICE Collaboration), *Phys. Rev. C* **92**, 054908 (2015).
 - [18] A. Bialas and K. Zalewski, *Phys. Lett. B* **727**, 182 (2013); A. Bialas, W. Florkowski, and K. Zalewski, *ibid.* **748**, 9 (2015).
 - [19] J. Rafelski, *Eur. Phys. J. A* **54**, 29 (2018).